Micro-Raman spectroscopic identification of natural mineral phases and their weathering products inside an abandoned zinc/lead mine

N. Goienaga [a]*, N. Arrieta [a] , J.A. Carrero [a] , M. Olivares [a] , A. Sarmiento [a,b] , I. Martinez-Arkarazo [a] , L.A. Fernandez [a] , J.M. Madariaga [a]

[a] Department of Analytical Chemistry, Faculty of Science and Technology, University of the Basque Country (UPV-EHU), P.O. Box 644, E-48080 Bilbao, Spain

b Raman-LASPEA Laboratory, SGlKer, Faculty of Science and Technology, University of the Basque Country (UPV-EHU), P.O. Box 644, E-48080 Bilbao, Spain

ABSTRACT

Mining activities provide a good source of minerals of different nature. On the one hand, the primary minerals for whose formation a geological time-scale is required. On the other hand, secondary minerals, formed from removed products after the earlier weathering and alteration states. These are characteristic of the local geology and the environment context that commonly appears due to the low chemical stability of their original primary minerals. This work shows how quickly the reactions promoting secondary minerals may have taken place, due to the fact that these were found in newly formed solid materials called efflorescences. To achieve this purpose, the sampling is crucial. It was carried out in such a way that tried to guarantee that the samples collected consisted in the very topsoil matter (first 2 cm depth). Thus, unlike the deeper soil, the material analysed may have been newly formed due to the interactions that they had with the place weathering agents (i.e. air oxygen, humidity, and microbial activities).

Raman spectroscopy has emerged as a good and fast non-destructive technique that provides molecular information of the local mineralogy without the need of any pre-treatment of the samples. At the same time, the work looked for information on the variety of non-stable lead and-or zinc containing minerals due to the possible heal th and environmental risks they convey. Among the different minerals identified, 16 were of primary nature while 23 may be classified as secondary minerals, probably formed in the last decades as the result of the extractive activities.

Keywords: *Raman spectroscopy, Lead, Zinc, Abandoned mine, Weathering, Efflorescences*

1. Introduction

Mineral formation is the result of a complex series of chemical reactions between the original rocks of a location and the sur- rounding dissolved ions and atmospheric gases. Without the formal rigor of Geological Mineralogy and in agreement with the literature [1-4], minerals may be included into two main groups: stable mineral phases (which will be signalled here as primary minerals), whose formation requires a geological time-scale and secondary minerals produced in the reactions that the original materials have with the environmental chemical and physical agents [1-4].

Mining wastes offer good examples for studying the conversion of primary minerals into unstable secondary products and other interactions caused by metal-rich solutions [5-7].

In mature soils where contamination arises from natural sources, the time of geo- logical evolution is much longer than in mine waste materials [8]. Although the texture, geometry, crystal structure and chemical composition of a mineral may influence its stability, the type and severity of the environment to which it is exposed could accelerate its alteration [9]. Therefore, other environmental factors such as temperature, humidity and pH become important to consider in order to understand better the behaviour of inorganic contaminants as well as the new mineral phases that may appear [10].

Heavy metals in different environmental compartments, like soils and sediments, have been often studied to predict their environmental risk [11]. In this sense, the runoff of the acid mine drainage (AMD) characteristic of abandoned mines and its impact on surrounding areas has been widely studied [12]. While the acid may be neutralized by the receiving water and/or the carbonate bedrock, some dissolved metals (Pb, Cu, Ag, Mn, Cd, Fe or Zn, among others) may remain in solution, leaking downstream or percolating through the soil column [13].

AMD is usually considered as a horizontal migratory movement of several heavy metals dissolved in the superficial waters that leak out from inside the mines. However, because of their vertical mobility, those dissolved trace metals may reach the groundwater, a situation that has been less studied than the previous one and which is characteristic of karstic environments due to their higher permeability [14]. These environmental contaminants may affect wildlife species in many ways and at many levels within the ecosystems and cause acute or chronic effects on resident wildlife [15].

Several methodologies are used to evaluate the bioavailability and mobility of such pollutants [16,17,15]. However, almost none of them provide information about new mineral phases formed as a consequence of the dissolution-precipitation processes: weathering of superficial mineral phases, percolation of dissolved ions and precipitation of new products as they move downwards. This phenomenon could be accelerated due to the increase of the atmospheric CO2 concentration and other acid gases (SOx, NOx). that reacts with the carbonate minerals producing dissolved bicarbonate anions and the corresponding soluble cations that can be re-precipitated as other species [18]. This kind of information may be obtained by Raman spectroscopy, a non-destructive technique that provides information about the molecular composition of the studied matter. Some authors have used this analytical technique to look for biogeochemical processes in sediments from the Antarctic Dry Valleys, as analogues of potential paleolakes on Mars [19], for in situ mineral identification of planetary surface analysis [20,21] or even on the seafloor [22], for assessing the impact of navigation acid gases emitted in an industrial harbour area affecting building stones [23], while other authors have used this technique for discerning between natural and anthropogenic species of the solid phases in sediments [10].

For a better understanding of the mobilisation process of minerals rich in toxic metals from the bedrock, the galleries of a zinc-lead mine (sulphide minerals in carbonate bedrock) abandoned 60 years ago have been sampled. The present work tries to determine the mineral composition related to the bedrock weathering using new non-compacted solid phases that are covering the rock materials of the walls as well as the soil of an abandoned mine's galleries. Thus, the transformation of the mineral composition under cave specific conditions (humidity, air oxygen, redox potential, etc. that changes yearly within the winter-summer cycles) must be investigated. Furthermore, this geochemical characterization may inform about the potentially adverse effects of some compounds stock in the studied

environment. Such information is of relevance due to the fact that the mine is situated in a karstic mountainous area, a type of geological outcrop characterized by high leaching capacity.

The determination of the mineral constituents, which are of interest in environmental monitoring, can be accomplished reasonably well using field portable equipment [24-26]. Nevertheless, due to the high environmental humidity inside the mine, field techniques cannot always provide the levels of detection and reliability obtained by well-established laboratory methods that make use of more sensitive spectroscopic equipment. Thus, the determination of the mineral composition was best done in the laboratory, using advanced spectroscopic techniques that include among other techniques, Raman vibrational spectroscopy on the dust sampled in different parts of the galleries. The Raman analysis at microscopic level of dust, where several mineral species can be simultaneously present, has been proven to be an effective analytical approach, both alone in highly sensitive materials like those belonging to the Cultural Heritage [27] or used together with other instrumental techniques in the analysis of dust collected from building stones [23].

2. Experimental

2.1. Studied area

As indicated in Fig. 1, the abandoned mine is located in the Karrantza Valley, the westerner area of the Basque Country (43º13'N; 3º26'W, North of Spain). There have been several activities related to the extraction of lead and zinc from sulphide ores situated in a mountainous karstic area (heights higher than 600 m above sea level) with an Acrisols Gelyic soil type [28].

In geological terms, the area has suffered two main formation phases. First a sedimentary process that created the original host rock followed by a hydrothermal progression. Such information may be completed according to the bibliography with the paragen-esis of the mineralization that is characteristic of this region, which comprises zinc and lead ores (mainly as sphalerite and galena) while the rock frame is calcite associated with quartz [29]. The present study is focused on the interior of the galleries belonging to an abandoned zinc blende (ZnS)-galena (PbS) mine, closed in the sixties of the last century. Even if the hill contains several galleries at different heights, due to the risks involved in sampling at these sites, only the main gallery was selected to take samples for analysis.

Due to the lack of activity since the mine's closing, the hillside has been colonized by various plant and animal organisms, resulting in what could be considered as an example of an industrial landscape becoming naturalized (natural alteration). However, a simple floristic study of the distribution of plants, which is not homogenous [28], gives an idea of the pollutant load that each area of the hillside supports due to the presence of dumps of washing materials.

2.2. Sampling procedure

The six sampling points selected were located along the first 30 m of the main gallery of the mine. The samples were collected in duplicate for each sampling point, one close to the ground and the other halfway up the wall of the gallery.

The analysed areas were under the same weathering conditions (i.e. lixiviation or redox potential conditions). As the temperature, humidity and ventilation were similar in those first 30 m, the pro- cesses that may take place can be considered the same.

The picked up samples were small pieces of stone/ mineral and dust, composed of non-compacted particles that were covering the original walls of the galleries or deposited in the soil of the gallery. Samples were stored in sterile sealed bags for transport. Once in the laboratory, they were dried on filter-paper (Resma ALBET®, 72 g m^{-2}) at room temperature.

The dried samples were sieved (Endecotts Octagon Digital) with two light-mesh sieves of 2 mm and 0.25 mm to separate the small rocks and grains. Afterwards they were stored in glass bottles at 4 °C until analysis in order to prevent microbial activity.

2.3. Instrumentation set-up

Molecular and elemental characterisation of the samples was carried out using non-destructive analytical techniques.

2.3.1. Raman spectroscopy

The molecular speciation of the samples was studied with two Raman Spectrometers: a Renishaw InVia and a Renishaw RA 100 System. The first one was attached to a Leica DMLM microscope. The spectra were acquired with a Leica 50x N Plan (0.75 aperture) long range objective. Besides, for the visualization and focusing, Leica 5x N Plan (0.12 aperture) and 20X N Plan EPI (0.40 aperture) objectives were used. The spatial resolution for the 50X objective is 2 μm. For the focusing and searching of the points of interest, the microscope implements a Prior Scientific motorised stage (XYZ) with a joystick.

The Raman scattering was obtained using a 514 nm (ion-argon laser, Modu-Laser) excitation source. The 514 nm laser has a nominal power at the source of 50 mW, being the maximum power at the sample of 20 mW. A holographic net of 1800 lines mm^{-1} was used.

The RA 100 Raman Spectrometer was coupled to a fibre optic micro-probe. The equipment has a 785 nm diode excitation laser, a Peltier-cooled CCD detector and a mobile diffraction grating of 1200 lines mm^{-1}. The laser has a nominal output power of 150mW at the source and filters allow working at 1%, 10% or 100% of the power. A monitored microprobe with built-in 20 x and 50x micro- scope lenses assisted by a colour UV micro-camera that allowed 40-60 μm focusing of the laser beam's spot was used to analyse the surface. The measurements resolution was of 1cm^{-1}.

Some kind of samples (i.e. sediments, soils) require the removal of the organic content for obtaining good spectra of the inorganic mineral phases [10], but in our case it was not necessary. Photobleaching was not applied for reducing the fluorescence or for gathering good signal-to-noise ratios.

In order to perform the spectroscopic analysis, a few milligrams of the sieved samples were set in a non-Raman active bed and extended along it for their measurement. Several spectra were obtained in different points of the same sample by focusing on different grains at a micron level. This procedure was repeated several times until approximately a hundred spectra per sample were collected. At least five Raman spectra were considered necessary to be collected for each mineral phase to claim its presence. Thus, the reported results may be considered representative of the mineral phases present in the samples.

Samples were scanned using a synchro-scan mode from 100 to 3200 cm-1 at a spectrum resolution of about 1 cm^{-1}. The acquisition time for each scan varied from 3 to 30 s, to obtain the best conditions for the analysed spot. However, in almost all of the measurements 10 s were enough. The number of accumulations varied from 3 to 30 in order to provide the best signal-to-noise ratios. Spectra were obtained using a 50x magnification objective while the laser power varied in intensity from 0.1% to 100% thanks to the filters used. Calibrations of the spectrometers were done at the beginning of each day and every 2 h using the 520.5 cm^{-1} line of silicon.

Raman data were handled with the Windows®-based Raman Environment software WiRE™, versions 2.0 and 3.0 (Renishaw, UK). Spectral analyses were performed by comparison with spectra from the in-house library e-VISNICH [30], an on-line Raman Spectra Database of Natural, Industrial and Cultural Heritage compounds (available at http:/1158.227.5.164/RamanDB/) and with a commercially available spectral library (Omnic, from Nicolet, Madison, WI, USA).

2.3.2. µ-ED-XRF

In order to check the presence of the metals found and complete the molecular Raman information, all the soil samples were subjected to elemental analysis by X-ray fluorescence spectroscopy.

These qualitative analyses were carried out using a portable Bruker ArtTax µ-ED-XRF equipped with an X-ray tube through molybdenum anode, working at a maximum voltage of 50 kV and a highest current of 0.6 mA. The X-ray fluorescence is detected by means of a thermoelectrically cooled Si-drift (XFlash) detector which has an active area of 5 mm2 and 8 µm beryllium window. The X-rays are collimated by a tantalum collimator with diameter of 0.65 mm and the beam diameter in the sample's surface is 200 μm^2. A CCD camera integrated in the measuring head gives an image of the sample surface (8 mm x 8 mm) and a motor-driven XYZ positioning unit allows focusing on different parts of the sample.

The samples were analysed directly in the particle size portion below 250 µm, without the need to do pellets. The operating conditions during the µ-ED-XRF measurements were fixed at 1000 s, at a voltage of 50 kV and a current of 0.5 mA. In order to detect lightweight elements a helium flow was used.

3. Results and discussion

The impact of atmospheric components (CO2 and O2, mainly), as well as biological activity (i.e. bacteria, lichen and moss), produce the continuous weathering of the bedrock materials. Part of the aqueous solutions after raining wash percolate through the bed rock after raining wash and penetrate in the inner part of the gallery cavities. When the pore waters appear in the walls of the cavity and evaporate, the solution containing the dissolved weathered ions is concentrated and may attain saturation conditions for most of the possible precipitates. Thus, new mineral phases are predictably formed in the surface, holes and cracks within the walls of the gallery as efflorescences [3]. Such considerations strengthen our sampling procedure (the first few centimetres of non-compressed matter collected from the galleries walls).

To ascertain the chemical composition of the studied samples, their elemental analysis was first carried out. As shown in Fig. 2, these measurements indicate exceptionally high concentrations of several heavy metals (i.e. Pb, Zn and Fe).

An exhaustive bibliographical review about the geological studies carried out in the studied area helped in the identification of the original mineralogical composition or paragenesis [29]. Nevertheless, to achieve this aim, big particle size soil fractions (over 250 μm) as well as rolling stones or rocks pieces chipped up from the walls were also analysed. They were mainly formed by dolomite and calcite (Table 1) in agreement with the karstic system of the Karrantza Valley together with zinc and lead ores (Tables 2 and 3). Considering that the solubilities and rates of mineral dissolution often increase by reducing their particle size (due to a higher reaction surface), together with the high environmental humidity inside the galleries, the chemical reactions mentioned above have resulted into several transitional mineral phases. These minerals were determined on the fraction below 250 μm.

Multiple spectra were obtained for each solid sample using the variety of optics described above, but it should be noted that both the spot orientation and location were not the same for each spectrum. As mentioned above, we set the criteria of recording at least five good spectra of any mineral phase were necessary to be recorded in order to claim for its sure presence in the samples. In consequence, the spectra shown in Figs. 3-6 are really representative of the different mineral phases found in the studied gallery, summarized in Tables 1-3.

Some spectra, such as hemimorphite (Fig. 3c), dolomite (Fig. 4e) or anglesite (Fig. 7b) are of excellent quality with good signal to noise ratios. Thus, these spectra were placed as new standards in our homemade database. However, in other cases not all of the bands were observed for each mineral, particularly when the ratios above mentioned were low. Sometimes not all the peaks were identified (i.e. Figs. 5 and 6), and in other cases the whole spectra could not be assigned. Such difficulty was maybe due to the lack of good quality standards or even to the possibility of the presence of numerous minerals with some of Raman bands merging among them. As it can be seen in Figs. 4-6, the information in the spectra found was explained by two or more minerals.

Although the present research was focused on those minerals related to the extracted ores (Zn and Pb) (Tables 2-3), the more commonly found minerals such as calcite, dolomite, magnesite or quartz were also included (Table 1). Those minerals marked with an asterisk are considered as natural or primary minerals while the rest are supposed to be secondary minerals formed as consequence of weathering processes.

Wavenumbers of the main Raman bands for the most frequently found minerals are summarized in Tables 1-3, together with their molecular formula and their assignment under the classification used during the present research. Fig. 4a, which shows the simultaneous presence of anatase and rutile, could be highlighted due to the fact that it is odd to be found in the consulted bibliography. Anatase represents one of three naturally occurring polymorphs of titanium dioxides and is characterised by a strong Raman band at 144cm-1 together with 198, 395, 513 and 634 cm^{-1} bands. Besides anatase, rutile was also widely detected among the samples, which is characterised by Raman bands at 240, 439 and 606 cm^{-1}. Thus, its simultaneous presence can be clearly detected by Raman spectroscopy.

The several elemental carbon forms observed during the analysis are commonly considered as primary minerals (i.e. solid bitumen, graphite and charcoal). The presence of these three occur- ring together in a rock type as primary minerals, is rather strange. However, such evidence matches up with the geological formation of the studied area, due to the fact that our system includes parts of rather sedimentary originating rocks as well as metamorphic ones [29].

Based on the bibliography, graphite is most commonly found in metamorphic rocks which have been altered under conditions of high temperature, and much of it derives from carbonaceous mate- rial of sedimentary origin. This agrees with the geological study of the iron and Pb-Zn-F mineralization in carbonated environments carried out in the University of the Basque Country (UPV-EHU) in 1982 by Herrero et al. [29].This is the reason why we classified such mineral as primary.

The spectra presented in Fig. 4b should also be commented because, apart from magnesite, the simultaneous presence of gypsum and anhydrite is clearly seen. Both are considered secondary minerals in other geological contexts. For instance, the gypsum solid phases present in the dust samples collected may have their origin in the evaporation of ion enriched water that leaks through the bedrock.

Apart from the carbonate primary minerals, the presence of fluorite and fluoroapatite could be considered the source for the fluoride and phosphate anions required to form some of the new mineral phases detected in this work. The complex tsumebite mineral (see Table 3) is a rare secondary mineral in the oxidised zone of some arsenic-bearing Pb-Cu deposits, with other lead-bearing phosphates and sulphates [31]. It may have its origin in the complex interaction among the metal-rich (i.e. Pb and Cu) AMD solution, the sulphate ions and the dissolved phosphates. From a geological point of view, it seems to be an odd mineral, which forms in dolomite or barite areas that are related to hydrothermal poly-metallic deposits [32]. The origin of the phosphate ions, however, may also be related to the fungi, bacteria or even to the plant decompositions (vegetal origin) [33] that leach across the soil column.

It is known that when bedrock materials are exposed to weathering agents (rain, snow, etc.) as well as to air gases (i.e. oxygen and carbon dioxide), the natural mineral composition changes following different chemical reactions. Thus, once the local carbonate and sulphurous species come into contact with the dissolved ions (i.e. metals, phosphates, sulphates, etc.) secondary mineral species such as zincite (Fig. 3b), anglesite (Fig. 7b) or tsumebite (Fig. Sb) are often formed.

Even if the exploited minerals were mainly those containing lead and zinc, the total amount of zinc minerals found was not as large as it could be expected (Table 2). The absence of zinc blende (ZnS) against the iron containing sphalerite should be also highlighted . Perhaps the iron enriched sphalerite [34] so commonly found did not have the same economical value due to the process- ing costs involved. At the studied area, this could be considered a secondary mineral rather than a primary one, resulting from dissolution, transportation and precipitation of zinc sulphides. However, we have classified it as a primary one due to the absence of zinc blende. This mineral is often associated with hemimorphite, a secondary mineral which nature could be explained by the same reason given for the smithsonite case, (i.e. by precipitation of zinc-rich hydrothermal solutions) [35]. Nevertheless, in this case both could be formed as the result of recent local reactions among dis- solved ions. The above mentioned smithsonite and hemimorphite sometimes

appear associated with rosasite, which origin has been also related to oxidation zones of copper and zinc deposits [36]. Thus, rosasite could also be pointed out as secondary mineral [37]. Besides minerals containing zinc, lead, cadmium or copper risky heavy metals, some arsenic compounds were also detected, i.e. leiteite. This last is a secondary mineral that is not easily reported is commonly used as reference material [38].

Although zincite can be a primary metamorphic mineral, due to the fact that in the analysed mine it was scarce, we have considered it as a secondary mineral, which origin can be found on the alteration of other minerals of zinc oxidized ores. The carbonated rain water that percolates through the soil may dissolve this zincite converting it into hydrozincite [39].

Despite the scarcity of zinc, lead was not either abundant in the studied area [40]. Nonetheless, the lead minerals were percentage- wise more common in the efflorescence materials sampled in this work (Table 3). The leaching of sulphate ions from the oxidation of sulphide minerals, in contact with calcium ion from the calcite bedrock, can explain the formation of gypsum (Fig. 4b) while the contact with lead-rich solutions may give as a result the anglesite (Fig. 7b). In the geosphere, the interactions in wet environments between calcite and anglesite rapidly generate gypsum and hydro- cerussite [41], so the same may occur inside our abandoned mine. Cerussite, so often associated with the sulphur and other secondary minerals such as goethite, anglesite or smithsonite, may appear at zones where the lead sulphide oxidises in the presence of the carbon dioxide gas-rich waters, as is the case studied. Often associated with it, is the dundasite [42], a mixed carbonate which origin may be related to the metal-rich solution that leaches through the studied karstic land and also through the abandoned galleries of the mine.

On the other hand, little is known about the mineral calderonite, which has also been found in Pb-Zn hydrothermal deposits else- where [43]. As in those cases, its origin may be explained by oxidation processes and further reaction of the dissolved ions.

The literature suggests the formation of heliohillite following a series of transformations from the original Pb oxychlorides. This may be also the origin of other secondary minerals quite often used as pigments, i.e. litharge [44] or even the native lead found in this work.

4. Conclusions

High quality Raman spectra were obtained from natural mineral samples using both red (785 nm) and green (514 nm) excitation lasers. Nevertheless, the highest quality spectra were obtained with green laser excitation and a sampling optic with a short depth of focus. Fluorescence was not significant, maybe owing to the high metal concentration together with the purity of the minerals.

As the minerals found in the present work were observed in the particle size fraction below 250 μm, the Raman ability to distinguish between mixed minerals is noteworthy . Once focused microscopically on a dust grain, more than a mineral may be detected, depending if the single crystal is or not bigger than the diameters of the laser spot. When the spot covered more than one single crystal, the spectra obtained showed more than one compound.

The distinctive paragenesis of the mineralisation of the Karrantza Valley remains unaltered inside the mine. Raman spectra of calcite, dolomite, galena, smithsonite, etc. were often obtained with high purity directly on the samples. As a consequence, such spectra were

subsequently introduced into our home-made database replacing the existing ones of lower quality. However, differences were found in the percentages of these minerals, as shown by the huge amount of secondary minerals appearing in most of the Raman spectra collected from the samples.

The transformation of primary minerals into secondary stable ones usually takes place along a geological time-scale. Nonetheless, such reactions are faster in areas were ore removal and mining activities alters the soil geology. Considering the short time that has elapsed since the abandonment of the mine, it is noteworthy that such solid phase changes have taken place at the studied area. A possible reason for these quick transformations may be found in some of the site is characteristics. On the one hand, the geological formation, a karstic environment with high permeability that allows an easy leaching of dissolved ions (mainly metals) from the top of the hill down to the studied galleries. On the other hand, the weathering agents (snow and rain, among others, containing acid substances) that affected it promoting possibly the reaction between different components, mobilising consequently dissolved ions through the bedrock. At this point the low pH value (around 4.2-4.8) of the snow which has been experimentally measured in the area during two consecutive winters should be taken into account because it affects directly the reactivity and solubility of the original mineral phases.

This hypothesis must be experimentally demonstrated and will be the subject of a forthcoming work that will consist in the analysis of samples for chemical and thermodynamic speciation in order to define the type of reactions among environmental stressors and original materials to form the new mineral phases found in this work.

Once the possible reactions that may have taken place are understood, the knowledge of the possible migration pathways of hazardous soluble ions throughout the soils and bedrock could be used to take the political actions to minimize the environmental risks associated to the abandoned mine surrounding.

Acknowledgements

This work has been financially supported by the ETORTEK Programme of the Basque Government through the BERRILUR III Project (ref. IE09-242). N. Goienaga, N. Arrieta and J.A. Carrero are grateful to the University of the Basque Country for their pre-doctoral fellowships. Authors are grateful to the facilities provided by the Raman-LASPEA laboratory (SGIKER), of the University of the Basque Country.

References

(1) Parfenova, E.A. Yarilova, V.V. Dokuchaev Inst. Soil Sci., Moscow 4 (1956) 38-42.

(2) A. Herre, F. Lang, Ch. Siebe, R. Dohrmann, M. Kaupenjohann, Eur. J. Soil Sci. 58 (2007) 431-444.

(3) F. Velasco, A. Alvaro, S. Suarez, J.M. Herrero, I. Yusta, J. Geochem. Explor. 87 (2005) 45-72.

(4) L. Haffert, D.Craw,J. Pope, N.Z.J. Geol. Geophys. 53 (2010) 91-101.

(5) J.B. Dixon, S.B. Weed, Minerals in the Soil Environment, 2nd ed., Soil Science Society of America, Madison, WI, 1989.

(6) D. Paktunc, A. Foster, S. Heald, G. Laflamme, Geochim. Cosmochim. Acta 68 (2004) 969-983.

(7) A. Aiuppa, W. D'Alessandro,C. Federico, B.Palumbo, M.Valenza,Appl.Geochem. 18 (2003) 1283-1296.

(8) M. Filippi, B. Doufova, V. Machovic, Geoderma 139 (2007) 154-170.

(9) E.M. Frempong, E.K. Yanful, Bull. Eng. Geol. Environ. 65 (2006) 253-271.

(10) U. Villanueva, J.C. Raposo, K. Castro, A. de Diego, G. Arana, J.M. Madariaga, J. Raman Spectrosc. 39 (2008) 1195-1203.

(11) Lui, B. Zhang, J. Cao, J. Domagalski, Ecotoxicology 18 (2009) 748-758 .

(12) A. Akcil, S. Koldas, J. Cleaner Prod. 14 (2006) 1139-1145.

(13) Jurjovec, C. Ptacek, D. Blowes, Environ.Sci. Technol. 37 (2003) 158-164.

(14) Deng, S. Wang, F. Li, Chin. J. Geochem. 28 (2009) 188-197.

(15) Wiater, A. Lukowski, Fresenius Environ. Bull. 19 (2010) 547-552.

(16) M.J. Jung, Sensors 8 (2008) 2413-2423.

(17) M.C. Reiley, Aquat. Toxicol. 84 (2007) 292-298 .

(18) K. Castro, M. Perez-Alonso, M.D. Rodriguez-Laso, N. Etxebarria, J.M.Madariaga, Anal. Bioanal. Chem. 387 (2007) 847-860.

(19) H.G.M. Edwards, S.E.J. Villar, J.L. Bishop, M. Bloomfield, J. Raman Spectrosc. 35 (2004) 458-462.

(20) S.K. Sharma, S.M. Angel, M.Ghosh, H.W.Hubble, P.G. Lucey, Appl. Spectrosc. 56 (2002) 699-705.

(21) L.A. Haskin, A. Wang, K.M. Rockow, B.L. Jolliff, R.L. Korotev, K.M. Viskupic, J. Geophys. Res. 102 (1997) 293-306.

(22) S.N. White, Chem. Geol. 259 (2009) 240-252.

(23) I. Martinez-Arkarazo, M.Angulo, L. Bartolome, N.Etxebarria, M.A. Olazabal,j.M. Madariaga, Anal. Chim. Acta 584 (2007) 350-359.

(24) I. Martinez-Arkarazo, D.C. Smith, 0. Zuloaga, M.A. Olazabal, J.M. Madariaga, J. Raman Spectrosc. 39 (2008) 1018-1029.

(25) Jehlicka, P. Vitek, H.G.M. Edwards, J. Raman Spectrosc. 41 (2010) 440- 444.

(26) M.A .Elbagerma, G. Azimi, H.G.M. Edwards, A.I. Alajtal, L.J. Scowen, Spectrochim. Acta A 75A (2010) 1403-1410.

(27) M. Perez-Alonso, K. Castro, M. Alvarez, J.M. Madariaga, Anal. Chim. Acta 524

(2004) 379-389.

(28) C. Garbisu, J.M. Becerril, L. Epelde, I. Alkorta, Ecosistemas AEET 16 (2007) 45-50.

(29) J.M. Herrero, F. Velasco, J.P. Fortune, Bol. Soc. Esp. Mineral. 5 (1982) 176- 178.

(30) M. Maguregui, N. Prieto-Taboada, J. Trebolazabala, N. Goienaga, N. Arrieta, J. Aramendia, L. Gomez-Nubia, A. Sarmiento, M.Olivares, J.A.Carrero, I. Martinez- Arkarazo, K. Castro, G. Arana, M.A. Olazabal, L.A. Fernandez, J.M. Madariaga, CHEMCH 1st International Congress Chemistry for Cultural Heritage, Ravenna, 30th June-3rd July, 2010.

(31) www.mindat.org website.

(32) W.D. Birch, Aust. Mineral. 5 (1990) 125-141.

(33) M.l. Makarov, L. Haumaier, W. Zech, O.E. Marfenina, L.V. Lysak, Soil Biol. Biochem. 37 (2005) 15-25.

(34) S. Kharbish, Phys.Chem. Miner. 34 (2007) 551-558.

(35) M.G.Yossifova, Coal Geol. 72 (2007) 268-292.

(36) R.L. Frost, D.L. Wain, W.N. Martens, B.J. Reddy, Spectrochim. Acta A 66 (2007) 1068-1074.

(37) R.L. Frost, Raman Spectrosc. 37 (2006) 910-921.

(38) R.L. Frost, S. Bahfenne, J. Raman Spectrosc. 41 (2010) 325-328 .

(39) F.M. Martins, J.M. dos Reis Neto, C.J. da Cunha, J. Hazard. Mater. 154 (2008) 417-425.

(40) M.J. Aguilar, Acta Geol. Hispanica 6 (1971) 92-96.

(41) A.G. Falgayrac, S. Sobanska, J. Laureyns, C. Bremard, Spectrochim. Acta A 64 (2006) 1095-1101.

(42) J.C. Moberly, T.Borch, R.K. Sani, N.F.Spycher, S.S. Sengor, T.R.Ginn, B.M. Peyton, Water Air Soil Pollut. 201 (2009) 195-208.

(43) J. Gonzalez Del Tanago, A. La Iglesia, j. Rius, S. Fernandez Santin, Am. Mineral. 88 (2003) 1703-1708.

(44) L. Burgio, R.J.H. Clark, S. Firth, Analyst 126 (2001) 222-227.

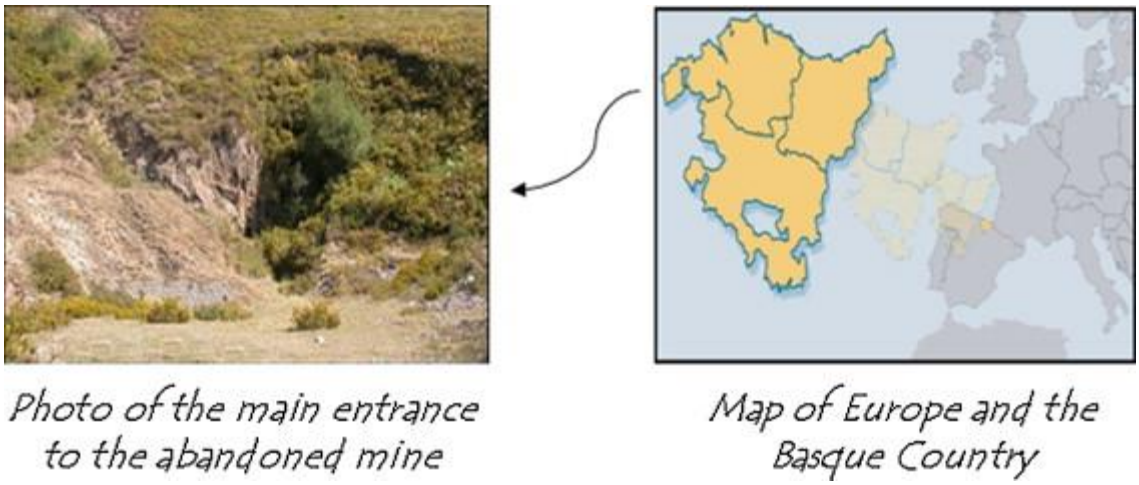

Fig. 1. Location of the studied abandoned mine.

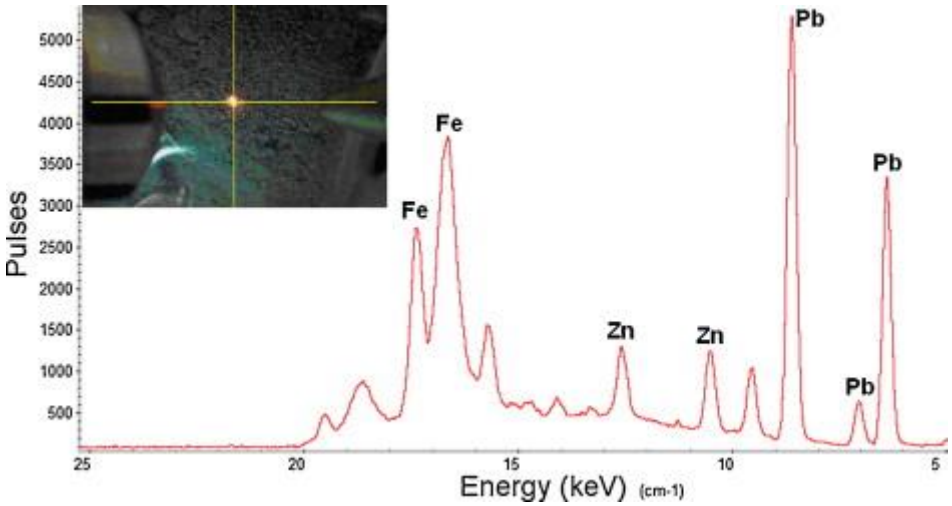

Fig. 2. XRF spectrum and its micro-image of one of the samples analysed.

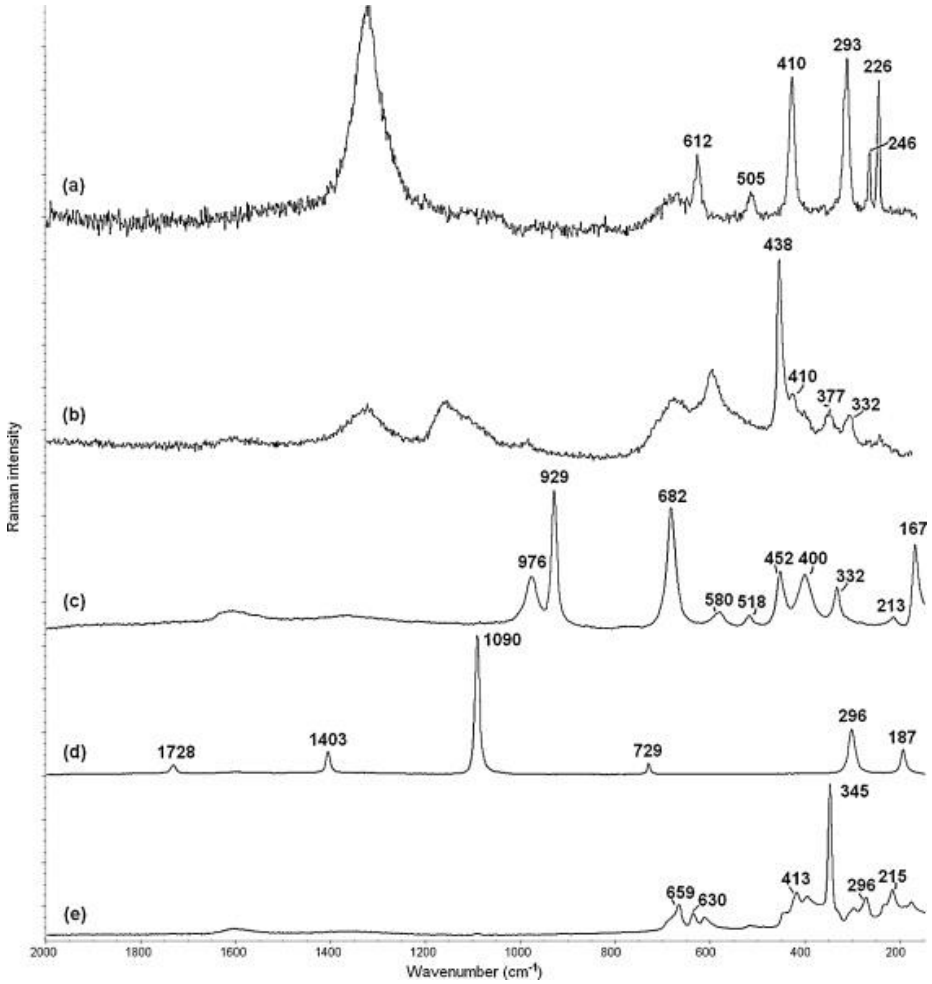

Fig. 3. Raman spectra of some pure minerals found containing Zn and their main wavenumbers: (a) versiliaite, (b) zincite, (c) hemimorphite, (d) smithsonite and (e) sphalerite.

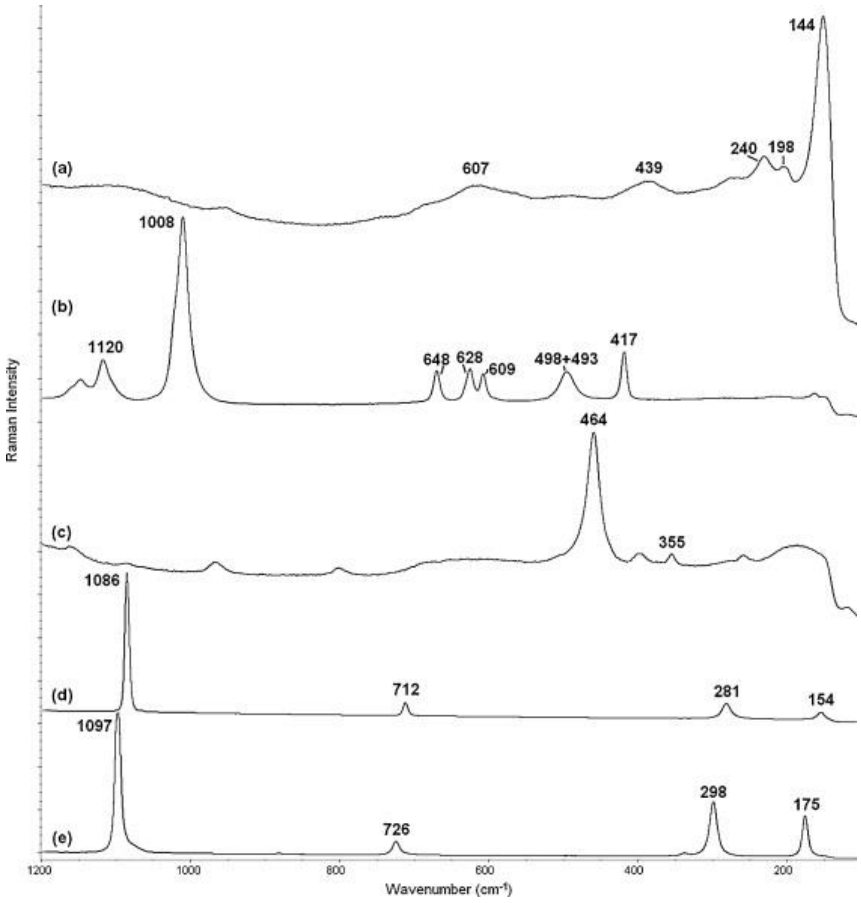

Fig. 4. Raman spectra of some local primary and secondary minerals found: (a) rutile (240 cm-1, 439 cm-1, 607 cm-1), anatase (144 cm-1, 198cm-1) ; (b) magnesite (1120 cm-1), gypsum (493 cm-1, 1008 cm-1), anhydrite (417 cm-1, 609 cm-1, 628 cm-1, 648 cm-1) ; (c) quartz; (d) calcite; (e) dolomite.

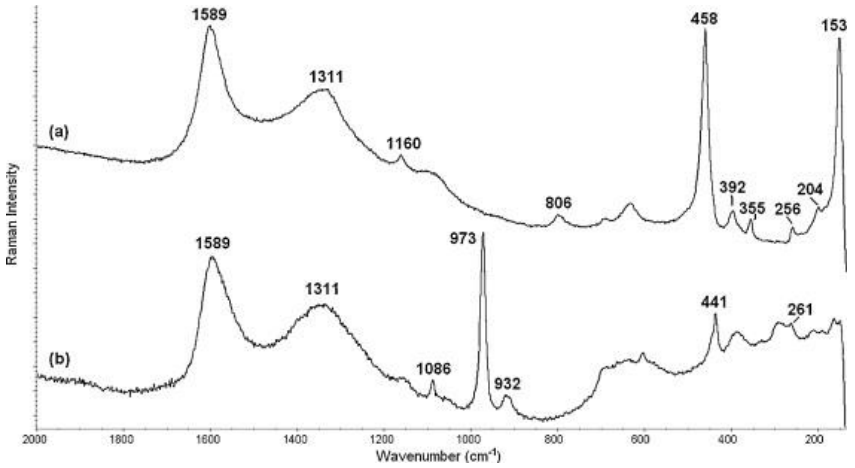

Fig. 5. Raman spectra of mixed mineral phases found: (a) charcoal (1311 cm-1, 1589cm-1); leiteite (256 cm-1, 458 cm-1, 806 cm-1); quartz (204 cm-1, 355 cm-1, 392 cm-1); lead (153 cm-1); (b) tsumebite (441 cm-1, 932 cm-1, 973 cm-1); charcoal (1311 cm-1, 1589 cm-1); barytocalcite (261 cm-1, 1086 cm-1).

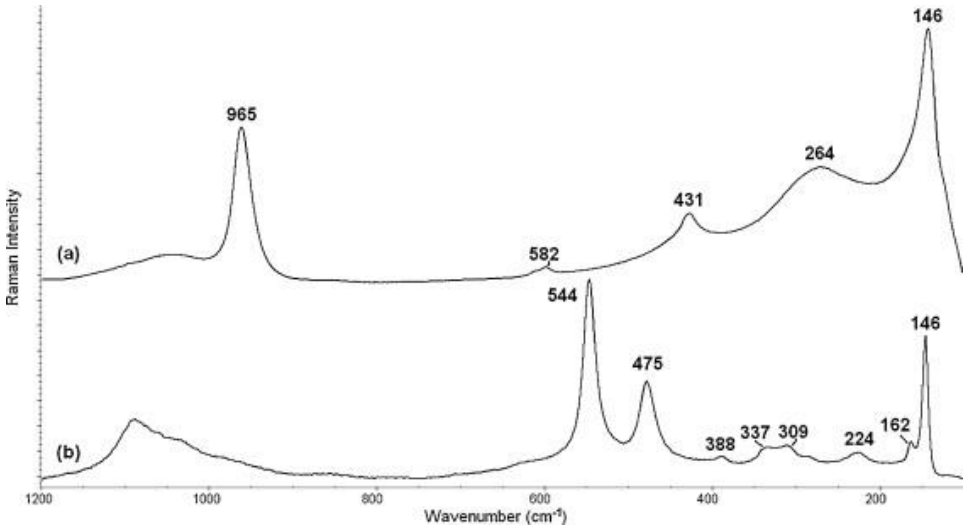

Fig. 6. Raman spectra of mixed mineral phases found :(a) apatite (431 cm-1, 582 cm-1, 965 cm-1), litharge (146cm-1), massicot (264 cm-1); (b) minium (162 cm-1, 224cm -1, 309 cm-1, 388 cm-1, 475 cm-1, 544 cm-1), litharge (146 cm-1, 337 cm-1).

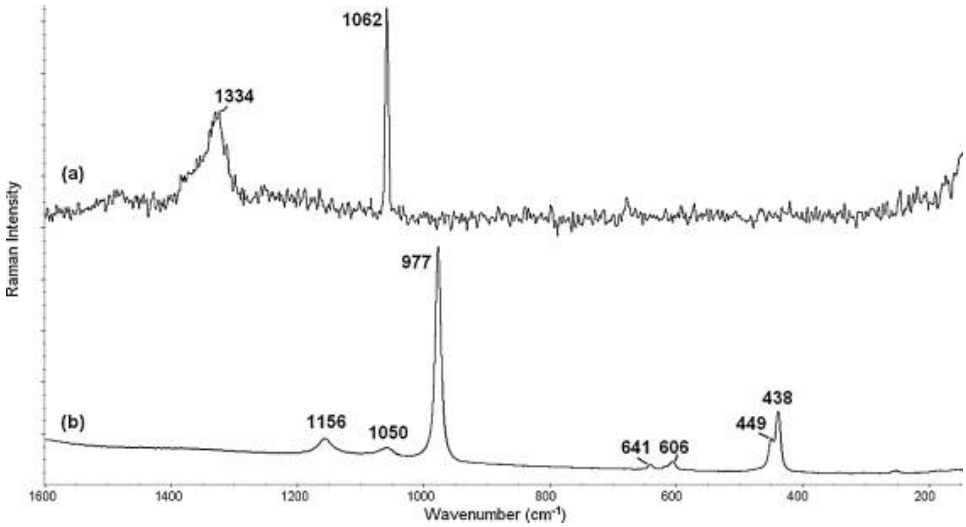

Fig. 7. Raman spectra of minerals found containing Pb: (a) cerussite and (b) anglesite.

Table 1. Principal Raman bands and molecular formula of the most frequently found minerals.

Mineral name	**Molecular formula**	***v*** **(cm^{-1}) (principal Raman bands)[a]**
Anatase[b]	TiO_2	634^{w}, 513^{s}, 395^{s}, 198^{vw}, 144^{vs}
Anhydrite0	$CaSO_4$	1160^{w}, 1130^{m}, 1017^{vs}, 648^{m}, 628^{m}, 609^{m}, 498^{m}, 417^{m}
Calcite[b]	$CaCO_3$	1748^{vw}, 1435^{vw}, 1086^{vs}, 712^{m}, 281^{m}, 154^{vw}
Barytocalcite	$BaCa(CO_3)_2$	1086^{vs}, 715^{vw}, 700^{vw}, 689.5^{vw}, 261^{w}, 224^{vw}, 200^{vw}, 107^{w}
Charcoal[b]	C	1589^{vs}, 1311^{s}
Dolomite[b]	$CaCO_3$	1758^{vw}, 1442^{vw}, 1097^{vs}, 726^{w}, 298^{m}, 175^{w}
Fluorite[b]	CaF_2	949^{vs}, 929^{s}, 913^{s}, 323^{s}
Fluorapatite	$Ca_5(PO_4)_3F$	1073^{m}, 1054^{vw}, 965^{vs}, 582^{w}, 431^{m}
Graphite[b]	C	1598^{vs}, 1355^{vs}
Gypsum	$CaSO_4 \cdot 2H_2O$	1135^{m}, 1008^{vs}, 670^{w}, 619^{w}, 493^{m}, 413^{m}, 116^{vw}
Magnesite[b]	$MgCO_3$	1120^{vs}, 1086^{vw}, 230^{w}, 201^{m}
Quartz[b]	SiO_2	1527^{m}, 1339^{vw}, 1160^{vw}, 747^{w}, 681^{w}, 464^{vs}, 392^{vw}, 355^{w}, 204^{m}
Rutile[b]	TiO_2	607^{vs}, 439^{s}, 240^{m}
Solid bitumen[b]	C	1583^{vs},1347^{s}

a) ^{vs}Very strong; ^{s}strong; ^{m}medium; ^{w}weak; ^{vw}very weak.
b) The minerals are considered as primary compounds in the studied area.

Table 2. Principal Raman bands and molecular formula of Zn or Cd minerals found.

Mineral name	**Molecular formula**	***v*** **(cm^{-1}) (principal Raman bands)[a]**
Hemimorphite	$Zn_4Si_2O_7(OH)_2 \cdot H_2O$	976^{m}, 929^{vs}, 682^{vs}, 580^{vw}, 518^{vw}, 452^{m}, 400^{m}, 332^{w}, 213^{vw}, 167^{s}
Hydrozincite	$Zn_5(CO_3)_2(OH)_6$	1061^{vs}, 736^{m}, 386^{s}, 231^{m}
Leiteite	$ZnAs_2O_4$	806^{vw}, 502^{w}, 458^{vs}, 256^{vw}, 219^{m}
Otavite[c]	$CdCO_3$	1086^{vs}, 808^{vs}, 268^{s}, 156^{m}
Greenockite	CdS	596^{m}, 298^{s}
Rosasite	$(Cu,Zn)_2CO_3(OH)_2$	1092^{vs}, 731^{w}, 302^{m}, 193^{m}
Smithsonite[c]	$ZnCO_3$	1728^{w}, 1599^{vw}, 1403^{m}, 1090^{vs}, 729^{w}, 296^{s}, 187^{w}
Sphalerite[b]	ZnS	659^{w}, 630^{vw}, 413^{vw}, 390^{vw}, 345^{vs}, 296^{m}, 215^{m}, 173^{w}
Versiliaite[b]	$(Fe^{2+},Fe^{3+},Zn)_8(Sb^{3+},Fe^{3+},As)_{16}O_{32}S_{1.3}$	612^{m}, 505^{w}, 410^{vs}, 293^{vs}, 246^{s}, 226^{vs}
Zincite[c]	ZnO	438^{vs}, 410^{vw}, 377^{w}, 332^{w}

a) ^{vs}Very strong; ^{s}strong; ^{m}medium; ^{w}weak; ^{vw}very weak.
b) The minerals are considered as primary compounds in the studied area.
c) Could be also a primary compound.

Table 3. Principal Raman bands and molecular formula of Pb minerals found.

Mineral name	**Molecular formula**	***υ*** **(cm^{-1}) (principal Raman bands)[a]**
Aikinite[b]	$CuPbBiS_3$	326^{s}, 227^{s}
Anglesite	$PbSO_4$	1156^{w}, 1050^{w}, 977^{vs}, 641^{vw}, 606^{w}, 449^{m}, 438^{m}
Calderonite	$Pb_2Fe(VO_4)_2(OH)$	977^{vs}, 684^{w}, 336^{m}, 210^{w}, 159^{m}
Cerussite[c]	$PbCO_3$	1334^{w}, 1062^{vs}, 846^{w}, 148^{m}
Cosalite[b]	$Pb_2Bi_2S_5$	439^{m}, 251^{s}, 140^{vs}
Dundasite	$PbAl_2(CO_3)_2(OH)_4{\cdot}H_2O$	1090^{vs}, 234^{s}, 193^{w}, 170^{s}, 152^{w}
Galena[b]	PbS	154^{vs}, 138^{vs}
Heliophyllite	$Pb_6As2O_7Cl_4$	808^{s}, 746^{s}, 718^{s}, 160^{vs}
Hydrocerussite	$Pb_3(CO_3)_2(OH)_2$	1050^{vs}, 969^{m}, 394^{m}, 271^{m}, 166^{m}, 127^{s},
Lead	Pb	153^{vs}
Litharge	PbO	337^{w}, 146^{vs}
Massicot	PbO	528^{vw}, 353^{vw}, 264^{s}, 134^{vs}
Minium	$Pb_2^{2+}OPb^{4+}O_4$	544^{vs}, 475^{m}, 388^{vw}, 309^{w}, 224^{w}, 162^{w}
Plattnerite	PbO_2	322^{vw}, 224^{vw}, 138^{vs}
Tsumebite	$Pb_2Cu(PO_4)(SO_4)(OH)$	973^{vs}, 932^{m}, 464^{s}, 441^{s}, 387^{w}
Zinkenite[b]	$Pb_9Sb_{22}S_{42}$	299^{s}, 282^{s}, 179^{s}

a) ^{vs}Very strong; ^{s}strong; ^{m}medium; ^{w}weak; ^{vw}very weak.
b) The minerals are considered as primary compounds in the studied area.
c) Could be also a primary compound.